ELSEVIER

Journal of Alloys and Compounds 228 (1995) 164–171

Journal of ALLOYS AND COMPOUNDS

Solubility and thermodynamics of hydrogen in homogeneous f.c.c. Pd–Pt alloys

H. Noh[a], Ted B. Flanagan[a], T. Sonoda[b], Y. Sakamoto[b]

[a]*Chemistry Department, University of Vermont, Burlington, VT 05405, USA*
[b]*Department of Materials Science and Engineering, Nagasaki University, Nagasaki 852, Japan*

Received 2 May 1995

Abstract

Hydrogen solubility data have been determined for homogeneous f.c.c. Pd–Pt alloys. In comparison with pure Pd, alloying with Pt leads to a decrease in the dilute phase hydrogen solubility at a given p_{H_2} and an increase of the plateau pressures. This makes this alloy–H system an exception to the classification of Pd alloys with regard to their hydrogen absorption behavior as contracted or expanded; the former type of alloys have lower dilute phase solubilities and greater plateau pressures than Pd, and the latter have larger dilute phase solubilities and lower plateau pressures. The enthalpies for hydrogen solution at infinite dilution of hydrogen do not change much with X_{Pt} but the corresponding entropies do change in such a way which would indicate that only interstices with six nearest neighbor Pd atoms are occupied. The enthalpies for hydride formation decrease in magnitude with X_{Pt}.

Keywords: Pd–Pt alloys; F.c.c. alloys; Hydrogen sorption; Hydride formation enthalpy

1. Introduction

Pd–Pt forms a continuous series of f.c.c. solid solution alloys. The substitution of Pt in the Pd lattice expands the Pd lattice slightly and therefore the alloy series should behave as 'expanded' with regard to hydrogen solubility [1]. This suggests that the Pd–Pt series should behave similarly to Pd–Ag alloys, i.e. the plateau pressure for hydride formation should decrease with increase of X_{Pt} and, at a given p_{H_2} in the dilute phase region, the solubility should increase with X_{Pt}. These trends would not be expected to be as great for the Pd–Pt alloys as for the Pd–Ag alloys because the lattice expansion is relatively small for the former. The solubility of hydrogen in Pd–Pt alloys has been investigated [2–4] and it was found that the plateau pressures increase rather than decrease with X_{Pt} and that the dilute phase solubilities decrease with X_{Pt} making this alloy system an exception to the lattice expansion/contraction classification of Pd-alloy behavior towards hydrogen. It was decided that it would be useful to re-examine this system in somewhat more detail.

2. Experimental

The alloys were in the form of thin foils. The thermodynamics of hydrogen solution were determined from pressure–composition–temperature (p–c–T) data. The data were determined in all-metal Sieverts' type systems which exist at the University of Vermont (USA) and at Nagasaki University (Japan). At Vermont the Pd–Pt alloys were routinely annealed by heating in air to reddish-white heat and then cooling or quenching into ice-water. This apparently crude technique gave identical hydrogen solubilities as annealing in vacuo in a furnace for prolonged periods of time at 1130 K followed by slow cooling.

3. Results and discussion

3.1. Solubility and thermodynamic parameters for the dilute phase

It has been found that the dilute phase solubility of Pd–Rh alloys is affected by the details of the anneal-

SSDI 0925-8388(95)01905-7

ing pretreatment [5]. This is because this alloy system has a miscibility gap and slow cooling causes some phase segregation which, in turn, affects the solubility. This limited phase separation which affects the hydrogen solubility is on a very fine scale and it is not detected in the X-ray diffraction patterns. In this research, the dilute phase hydrogen solubility was measured for two forms of an alloy of stoichiometry $X_{Pt} = 0.10$. One was prepared by quenching into ice-water from an elevated temperature and the other by slow cooling in a massive air furnace. Detectable differences in the dilute phase solubilities were not observed between the two forms of the alloy (Fig. 1). This is an indication that the Pd–Pt alloys do not have a miscibility gap, as do the Pd–Rh alloys.

Pd-rich alloys have two-phase plateau pressures whose characteristics depend upon the composition and the specific alloying metal [6,7]. It has been reported in recent studies of hydrogen absorption by Pd–Rh and Pd–Ni alloys that the plateau pressures evolve with cycling through the hydride phase change at moderate temperatures [8–10]; the plateau pressures for hydride formation decrease and for hydride decomposition increase leading to a decrease in the extent of hysteresis, i.e. $1/2RT(p_f/p_d)$, where p_f and p_d are the formation and decomposition plateau pressures respectively. It has also been shown recently how cycling can affect the van't Hoff plots and the derived thermodynamic parameters for the plateau reaction using the Pd–Ni–H system to illustrate the effect [10]. It is of interest to investigate how cycling affects the plateau pressures for Pd–Pt alloys.

The plateau is not very extensive for the $X_{Pt} = 0.10$ alloy and therefore the dilute phase solubility and the plateau pressures should not be much affected by 'cycling' through hydride phase formation and decomposition. The $X_{Pt} = 0.10$ alloy was cycled consecutively at 273 K and the dilute phase solubility was measured after 1, 2, 3, 4, 9, 14, 21 and 28 cycles. Between each isotherm measurement the alloy was evacuated at 273 K for several hours. In Fig. 1 (273 K) the solubilities after 1, 2 and 28 cycles are shown. The solubility enhancement after 1 cycle is smaller than that observed after 1 cycle for Pd, but the alloy's solubility continues to increase with cycling whereas it tends to saturate after fewer cycles for Pd. Also shown in Fig. 1 is the dilute phase solubility for the alloy after cold-rolling. The solubility enhancement for the cold-rolled form is similar to that for the annealed foil after its second cycle, except in the region near the beginning of the plateau where the cycled form shows a greater solubility (Fig. 1).

In order to determine thermodynamic parameters for the dilute phase, the solubilities were determined with alloys which had been annealed and then had never formed hydride phase. Typical dilute phase solubilities are seen for a series of alloys at 303 K in Fig. 2, where it can be seen that at a given equilibrium pressure of hydrogen in the dilute phase the hydrogen solubilities decrease with increase of X_{Pt}. Judging from

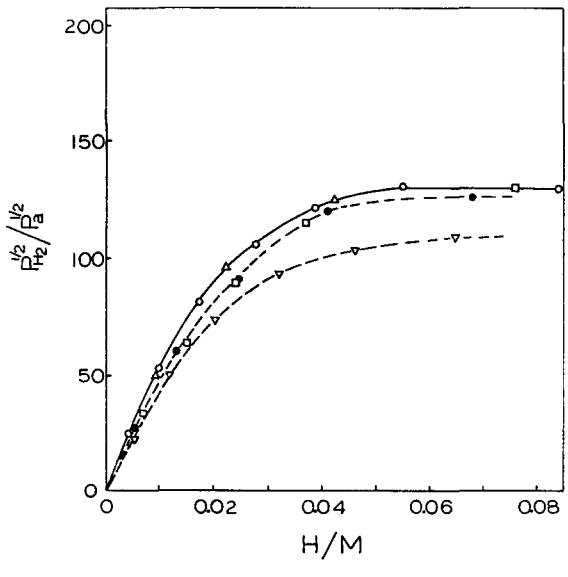

Fig. 1. Dilute phase hydrogen solubility data for $X_{Pt} = 0.10$ at 273 K: △, ice quenched form; ○, sample annealed in furnace and cooled at about 100 K h^{-1}; ●, solubility after a single complete cycle of hydriding at 273 K; ▽, solubility after 28 cycles of hydriding; □, cold-worked form.

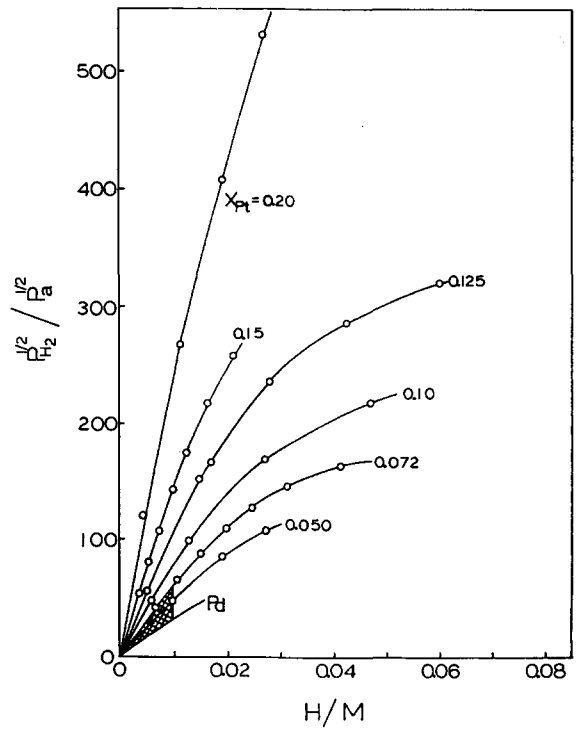

Fig. 2. Isotherms at 303 K for Pd–Pt alloys in the annealed, virgin form. The crosshatched area corresponds to the initial solubility range of all the alloys after correction for the available fraction of interstitial sites, as explained in the text.

plots made of $r(=H/M)$ or $\ln r$ against X_{Pt} at a constant value of p_{H_2}, it is clear that the latter is linear but not the former; this is because it is related to a thermodynamic parameter but the former is not. The solubility behavior can be described by [11]

$$\frac{1}{2}RT\ln p_{H_2} = \Delta\mu_H^o + RT\ln(r/(1-r)) + \mu_H^E(r) \quad (1)$$

where μ_H^o and μ_H^E are the chemical potentials of hydrogen at infinite dilution of H and the excess or non-ideal contribution respectively. At constant p_{H_2}, the relation between $\ln r$ and alloy composition can be seen from a rearrangement of Eq. (1) which is valid at small r, i.e.

$$RT\ln r = -\Delta\mu_H^o = -\Delta H_H^o + T\Delta S_H^o \quad (2)$$

Of the two terms on the right-hand-side of Eq. (2) the last one varies nearly directly with X_{Pt} (Table 1); this explains the observed linear dependence of $\ln r$ upon X_{Pt}. The first term on the right-hand-side does not change very much X_{Pt} (Table 1). The thermodynamic parameters for hydrogen solution in the dilute phase were determined in two different ways. Eq. (1) can be rearranged to give

$$RT\ln p_{H_2}^{1/2}((1-r)/r) = \Delta\mu_H^o + \mu_H^E(r) \quad (3)$$

If the left-hand-side is plotted against r, straight line behavior is found for small values of r because $\mu_H^E(r) \approx g_1 \times r$. The intercepts of such plots give $\Delta\mu_H^o$ values because $\mu_H^E \approx g_1 \times r$ vanishes as $r \to 0$. If the values of $\Delta\mu_H^o/T$ obtained from the intercepts at various temperatures are plotted against $1/T$, the slopes give ΔH_H^o and the intercepts ΔS_H^o. It should be noted that in Eq. (1) it has been implicitly assumed that all of the octahedral interstices are available for hydrogen occupation, i.e. in the denominator of the configurational entropy term the interstices accessible to hydrogen is given as $r = 1$. If this is incorrect, it will be reflected in the values of ΔS_H^o, i.e. they will be more negative than would be found if the 1 in the denominator were to be replaced by the fraction of available interstices β in the configurational term of Eq. (1).

The ΔH_H^o and ΔS_H^o thermodynamic parameters can also be determined from plots of $\Delta\mu_H/T$ against $1/T$ at a series of different values of r. These plots give values of ΔH_H^o and ΔS_H^o. If ΔH_H^o and ΔS_H^o thermodynamic parameters are extrapolated to $r = 0$, ΔH_H^o and ΔS_H^o can be obtained from the values found at infinite dilution of hydrogen. The two methods should give closely similar results; the results are shown in Table 1 where β (Eq. (1)) has been assumed to be 1.

The enthalpies at infinite dilution are seen from Table 1 to be nearly constant with X_{Pt} (Fig. 3). The values determined at the University of Vermont and Nagasaki University agree very well, and it should be repeated that different samples and apparatuses were

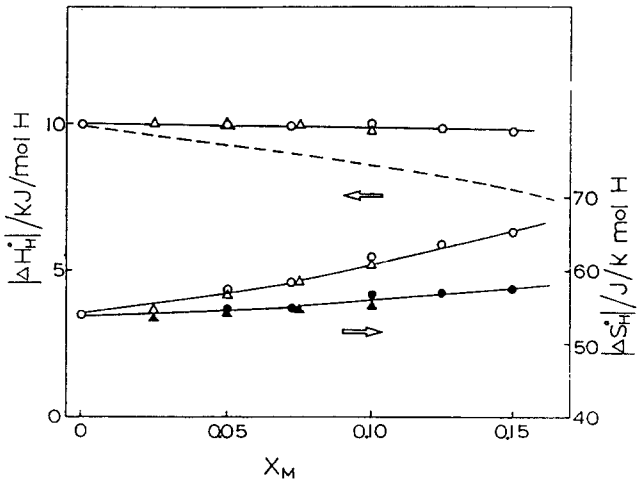

Fig. 3. Thermodynamic data at infinite dilution for annealed alloy forms: ○, data obtained at the University of Vermont; △, data obtained at Nagasaki University. The filled symbols have the same meaning but they represent values of ΔS_H^o after correction for the fraction of available interstices. The dashed line corresponds to data for Pd–Rh alloys [5].

Table 1
Thermodynamic quantities for hydrogen solution in Pd–Pt alloys derived from p–c isotherms. ΔH_H and ΔS_H values are in kJ (mol $\frac{1}{2}H_2$)$^{-1}$ and J K^{-1} (mol $\frac{1}{2}H_2$)$^{-1}$ respectively. The units of g_1 are kJ (mol $\frac{1}{2}H_2$)$^{-1}$

Alloy X_{Pt}	a_0 (nm)	$-\lvert\Delta H_H^o\rvert$	$-\lvert\Delta S_H^o\rvert$	$-g_1$
0.0	0.3889	10.0	54	[54]
0.025	—	[10.08]	[54.8]	[44.4]
0.05	0.3890	9.93,[10.01]	57.5[56.7]	41.3[40.7]
0.072	—	9.88	58.6	36.9
0.10	0.3891	10.05(9.84),[9.71]	61.5(62.1),[60.63]	41.8[37.1]
0.125	—	9.70(9.80)	62.8(63.0)	39.3
0.15	—	9.72(9.7)	65.25(65.2)	32.4

The a_0 data for Pd–Pt alloys from Ref. [12] and the values for pure Pd–H are taken from reference [13]. The thermodynamic values for infinite dilution from alloys employed at the University of Vermont shown in brackets refer to those obtained from the extrapolation of plots of ΔH_H against $r \to 0$ and those without parentheses are obtained from plots of $\Delta\mu_H^o/T$ against $1/T$. The values of ΔS_H^o have been calculated assuming that β in Eq. (1) is 1. The values with and without brackets refer to data obtained at Nagasaki University and the University of Vermont respectively.

employed in the two investigations. For contrast, the enthalpies for the Pd–Rh systems are also shown in Fig. 3, where it can be seen that the magnitudes decline with X_{Rh}.

The entropies at infinite dilution when evaluated using $\beta = 1$ appear to decrease with X_{Pt} as seen in Fig. 3, where again there is good agreement between the two independent determinations. When the entropies are evaluated assuming that $\beta = X_{[Pd_6]}$ where $[Pd_6]$ is the fraction of interstices surrounded entirely by Pd atom nearest neighbors, ΔS°_{H} becomes nearly constant (Fig. 3). The fraction of such interstices is calculated using the binominal theorem, i.e. $\beta = X^{6}_{Pd}$, which assumes that the alloys are random, disordered alloys. This is reflected by the range shown as the crosshatched area (Fig. 2) which shows adjusted dilute phase solubilities near the origin. The crosshatched area represents the range of the solubility data if the solubilities are corrected for the fraction of available interstices, i.e. by multiplying the observed hydrogen solubilities by X_{Pd_6}. The fact that the solubilities are all rather similar after the correction illustrates that a large part of the solubility behavior of these alloys can be accounted for by the fraction of sites available for hydrogen occupation in each alloy.

The excess hydrogen chemical potential, $\mu^{E}_{H}(r)$, can be approximated by a linear dependence upon r at small r as noted above, $\mu^{E}_{H}(r) \approx g_1 \times r$. When data for the alloys are plotted according to Eq. (3), the slopes correspond to the linear coefficient at small r. The average of values for different temperatures are shown in Table 1. Sakamoto et al. [14] have recently reported values of $g_1 = -38.3$ kJ (mol $1/2H_2)^{-1}$ ($X_{Rh} = 0.05$) and -30.6 kJ mol $1/2H_2$ ($X_{Rh} = 0.10$) for some representative low Rh content alloys. For Pd–Ag alloys the linear coefficient, $|g_1|$, also falls with solute content [15]. Thus the trend appears to be independent of whether or not the alloy belongs to the contracted or expanded category.

3.2. Solubility in the concentrated range

3.2.1. The effect of cycling on the plateau pressure of the $X_{Pt} = 0.10$ alloy

The effect of cycling on the plateau pressures of the $X_{Pt} = 0.10$ alloy is shown in Fig. 4. Both plateau pressures for hydride formation and decomposition slowly decrease with cycling and, after 15 cycles, they both fall below the initial decomposition plateau. They continue to fall with further cycling and, after 28 cycles, the plateaux have both fallen to below the decomposition plateau found after 15 cycles (Fig. 4). Hysteresis is still present after 28 cycles, but it is very small compared with its initial value (Fig. 4). The hydrogen capacity is unchanged by cycling, i.e. the

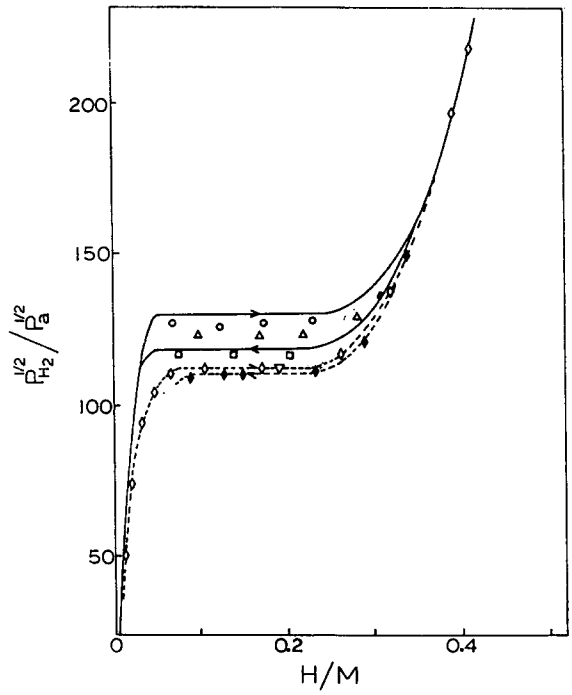

Fig. 4. Figure showing isotherms for the $X_{Pt} = 0.10$ alloy resulting from repeated hydriding and dehydriding (cycling) at 273 K. The continuous curves show the initial cycle; ○, cycle 2; △, cycle 4; □, cycle 9; ▽, cycle 28; ◊, cycle 28. The dashed lines are drawn through the cycle 28, and the open and filled symbols refer to absorption and desorption data respectively.

value of r corresponding to the steeply rising part of the isotherm where the limiting hydrogen content for this pressure range is approached.

The isotherms for each alloy system are affected by cycling but the specific effects differ between the various systems [8,9]. The effect of cycling is found to always increase with X_M but, when different systems are compared, the effects become significant at different values of X_M; for example, for Pd–Ni the effects are significant for $X_{Ni} = 0.10$ [9], whereas for Pd–Rh comparable effects do not appear until $X_{Rh} = 0.15$ [8]. For pure Pd the effects of cycling are minimal [16]. It should also be noted that the effects of cycling have been found to be similar for various forms of a given Pd-alloy, i.e. cold-rolled, annealed, and melt-spun. The microstructures of these various alloy forms differ, and yet the results of cycling on the isotherms are similar for all forms for a given composition [16].

The origin of the cycling effect seems to be connected with long range stress fields as modified by the solute atoms; the stress fields arise from hydride formation and decomposition and they evolve during the cycling. It should be noted that hydriding and dehydriding causes the formation and movement of dislocations [17,18]. The details of cycling in Pd alloys remain obscure, but it is an important effect because

the plateau thermodynamic properties are important for technological applications. It should be noted that non-Pd based binary alloys will probably also exhibit effects of cycling, but this has not been investigated in any other alloy systems; large differences of plateau pressures for hydride formation are observed between the initial and subsequent isotherms for the hydriding of intermetallic compounds [19–21].

3.2.2. Complete isotherms for annealed Pd–Pt alloys

In order to avoid effects due to cycling, only annealed, 'virgin' alloys were employed for the measurement of complete isotherms. Fig. 5 shows a comparison of isotherms for Pd–Pt alloys at 273 K. It can be seen that the hydride phase no longer forms for $X_{Pt} > 0.125$. The breadth of the plateau region decreases with increase of X_{Pt}, and hysteresis is seen to decrease with increase of X_{Pt} (Table 2). The relationship between $\ln p_{plat}$ and X_{Pt} is quite linear. Despite the absence of two phases in the $X_{Pt} = 0.15$ alloy, it dissolves appreciable hydrogen at higher pressures e.g., $r = 0.3$ at 273 K.

Complete absorption isotherms at different temperatures for alloys with compositions $X_{Pt} = 0.025$, 0.05 and 0.10 are shown in Figs. 6–8. Data at different temperatures have also been determined for 0.075 and 0.125 but are not shown. Van't Hoff plots have been constructed from the plateau pressures such as those shown in Figs. 6–8, and these have been employed to

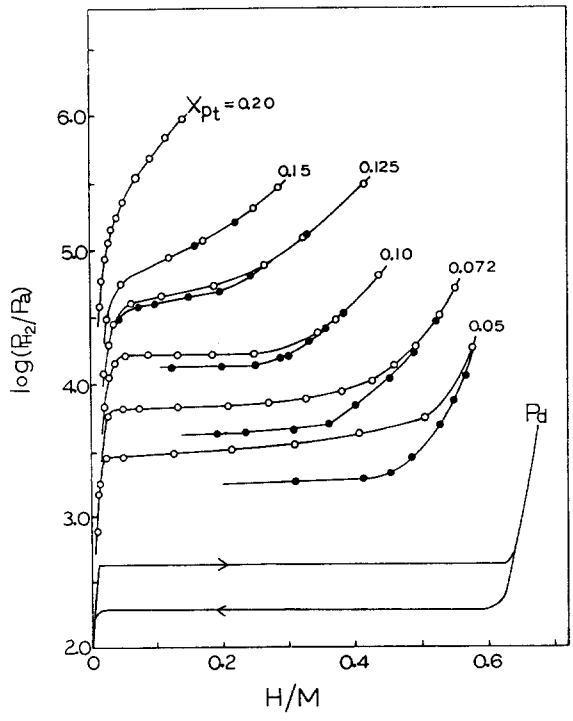

Fig. 5. Isotherms (273 K) for well annealed Pd–Pt alloys. The open and filled symbols refer to absorption and desorption data respectively. The isotherms are each labeled with the atom fraction of Pt.

Table 2
Thermodynamic parameters for hydrogen in Pd–Pt alloys derived from p–c isotherms. Hysteresis is evaluated as $\frac{1}{2}RT\ln(p_f/p_d)$ in units of kJ (mol $\frac{1}{2}H_2)^{-1}$; ΔH_{plat} and ΔS_{plat} values are in kJ (mol $\frac{1}{2}H_2)^{-1}$ and J K^{-1} (mol $\frac{1}{2}H_2)^{-1}$ respectively

Alloy	Hysteresis (283 K)	$\lvert\Delta H_{plat}\rvert$	$\lvert\Delta S_{plat}\rvert$
0.025	–	[17.5]	[45.7]
0.05	760	16.5(18.5),[16.4]	46.2(50.8),[46.0]
0.072	400	15.9(17.7)	47.3(51.6)
0.10	210	13.9(15.3),[13.2]	43.3(46.9),[42.6]
0.125	140	118(12.65)	40.8(43.3)
0.15	—	—	—

The values for the plateau quantities with and without parentheses refer to desorption and absorption respectively, determined at the University of Vermont for the fast-quenched forms of the alloys. The values in brackets refer to absorption plateau values determined at Nagasaki University.

determine plateau thermodynamic parameters, i.e. those corresponding to

$$\frac{1}{2}H_2(g) + \frac{Pd_{1-x}Pt_xH_a}{(b-a)} \rightarrow \frac{Pd_{1-x}Pt_xH_b}{(b-a)} \quad (4)$$

where a and b are the H/M ratios for the co-existing dilute and hydride phases and $x = X_{Pt}$. The van't Hoff plots were for the absorption plateaux data taken in Nagasaki (Figs. 6–8) and for both absorption and desorption plateaux data taken in Vermont. Results are shown in Table 2 and Fig. 9.

It can be seen in Table 2 and Fig. 9 that, in contrast to the enthalpies at infinite dilution (Table 1) which are nearly unchanged with X_{Pt}, the plateau enthalpies decrease in magnitude with X_{Pt} leading to the observed increase in the plateau pressures. Fig. 9 shows that the plateau entropy values are nearly constant with X_{Pt}.

The relationship between ΔH_{plat} and X_{Pt} is not a linear one but it is interesting that the relation between $\Delta\mu_{plat}(= 1/2RT\ln p_{plat})$ and X_{Pt} is linear. Normally, for most Pd alloy systems, if values of ΔH_{plat} decrease in magnitude with solute concentration, then there is a concomitant decrease in the values of ΔH°_{H}. For example, for the Pd–Ni alloys [22] the values are $X_{Ni} = 0.05, -9.5(-16.6)$, $X_{Ni} = 0.096, -7.9(-13.5)$, $X_{Ni} = 0.15, -6.0(-11.5)$ where the values without parentheses are for ΔH°_{H} and those with parentheses are for ΔH_{plat} in units of kJ (mol $1/2H_2)^{-1}$.

The hydrogen contents at the end of the plateaux for the Pd–Pt alloys are rather small compared with the same alloy compositions of some other substitutional alloys of Pd. For example, for the $X_{Pt} = 0.10$ alloy, r at the $(\alpha+\beta)/\beta$ boundary is only about 0.25 at 303°C (Fig. 8). By comparison for this same composition, the r values at the end of the plateaux contents at 303 K are 0.43 for Pd–Ag [15], 0.40 for Pd–Cu [23] and 0.47 for Pd–Ni [16].

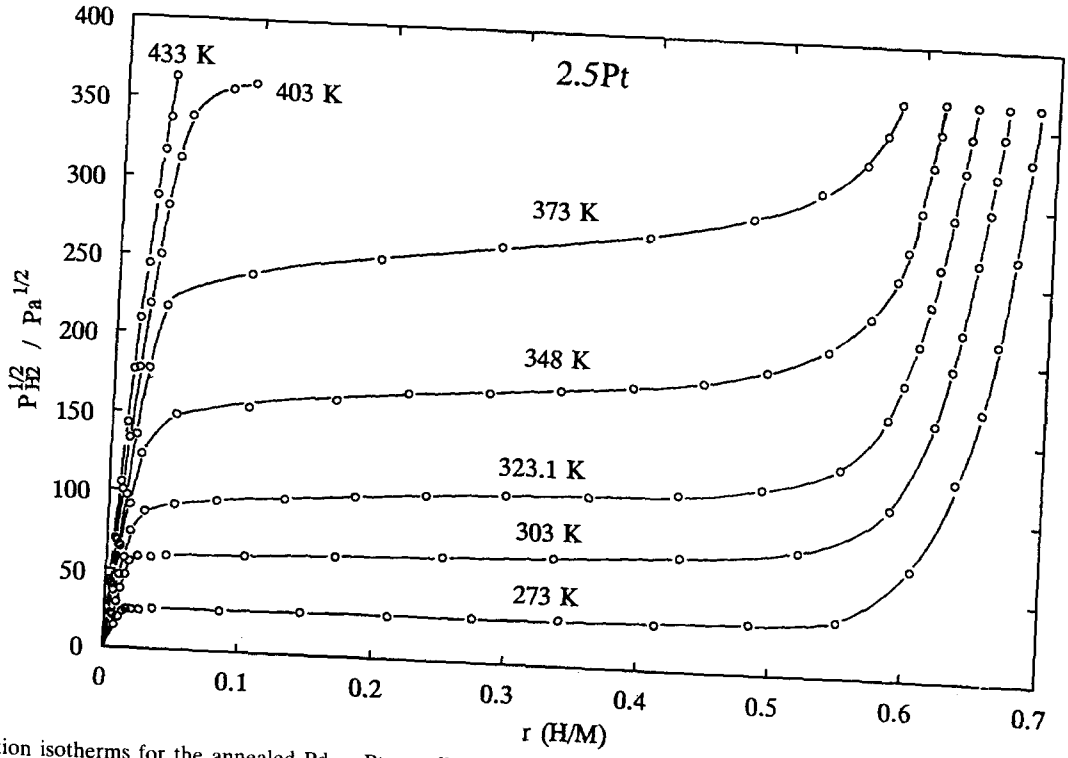

Fig. 6. Absorption isotherms for the annealed $Pd_{0.975}Pt_{0.025}$ alloy.

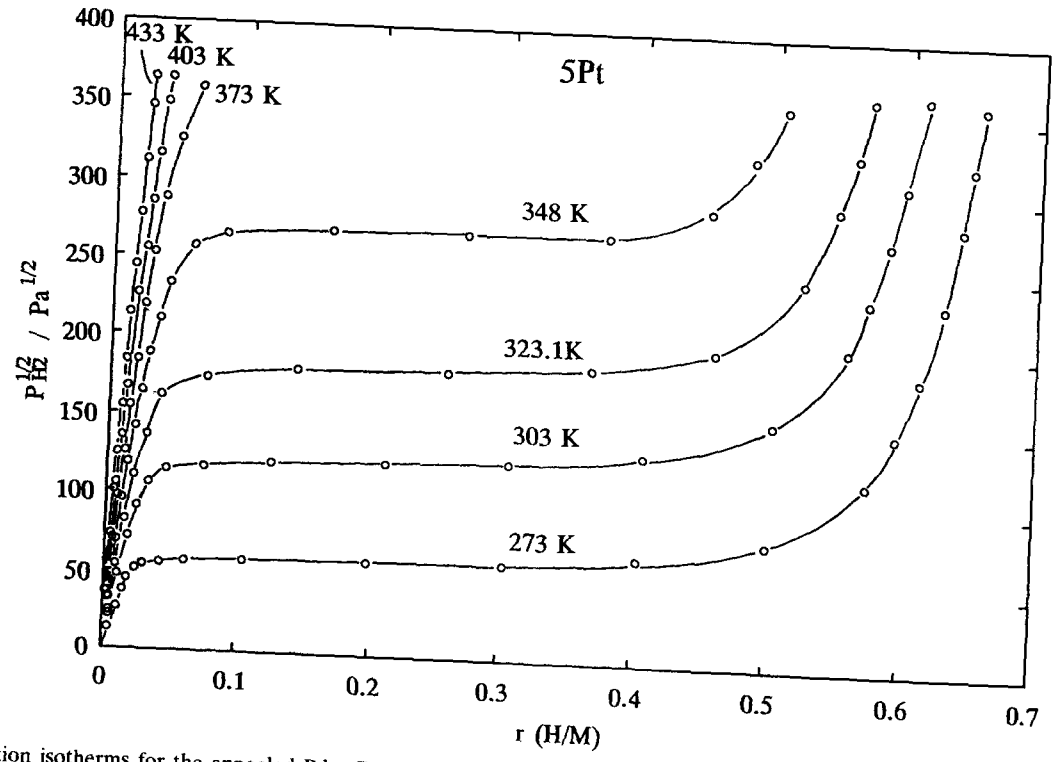

Fig. 7. Absorption isotherms for the annealed $Pd_{0.95}Pt_{0.05}$ alloy.

4. Conclusions

It is of interest that ΔH_H° does not change very much with X_{Pt}. The reason for this is presumably because the lattice parameter of Pd does not change very much by alloying with Pt (Table 1); if the hydrogen enters only the $[Pd_6]$ interstices, then their size and chemical nature are similar to those occupied in pure Pd. The

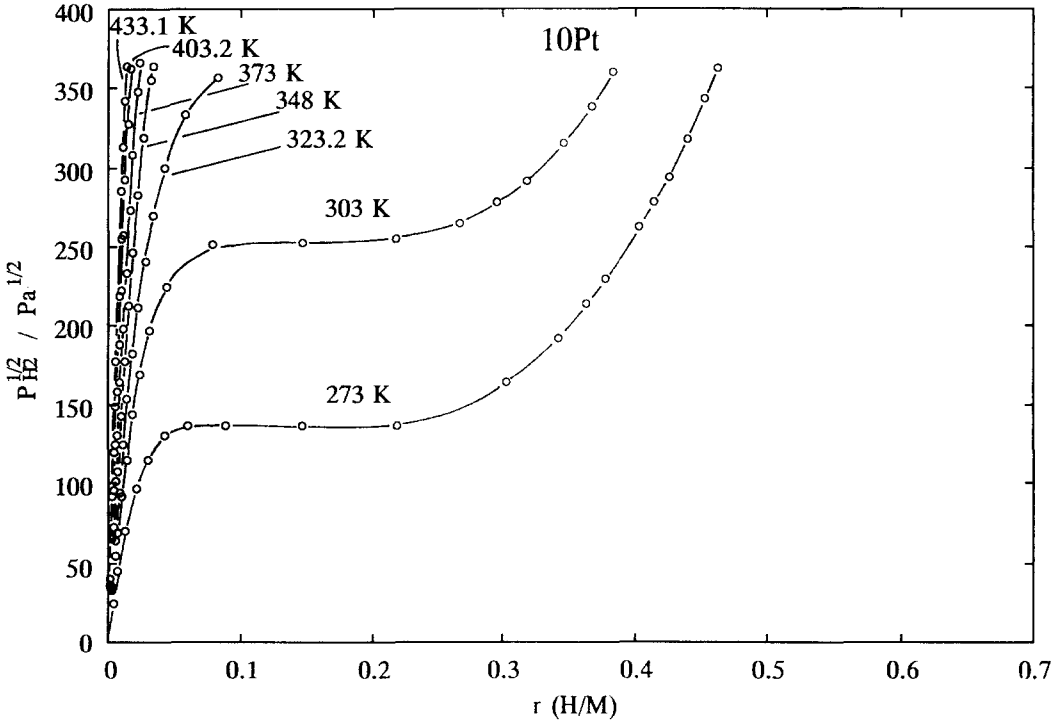

Fig. 8. Absorption isotherms for the annealed $Pd_{0.90}Pt_{0.10}$ alloy.

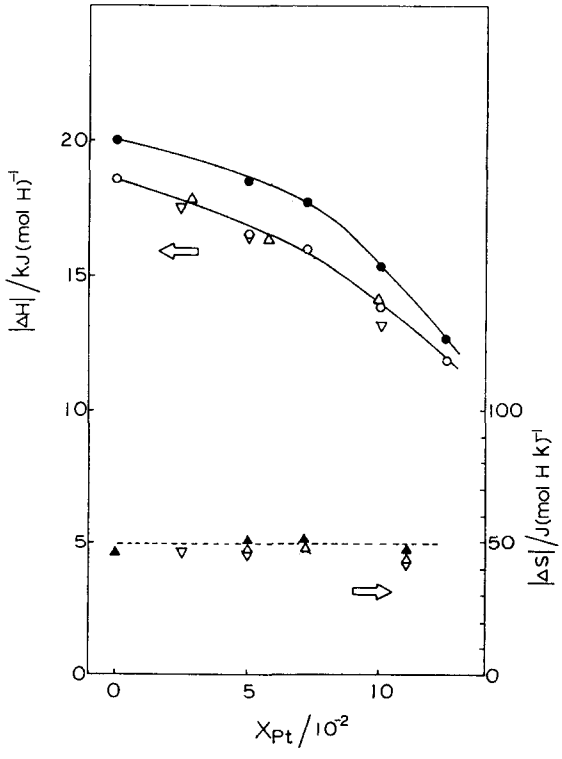

Fig. 9. Plateau thermodynamic data for annealed Pd–Pt alloys: ○, data obtained at the University of Vermont; ▽; data obtained at Nagasaki University; △, data from Ref. [24]. The open and filled symbols refer to absorption and desorption data respectively.

occupation of the $[Pd_6]$ interstices as $r \rightarrow 0$ is consistent with the entropy results. The values of ΔH_{plat}, however, decrease in magnitude with increase of X_{Pt} (Table 2) even though it is possible that hydrogen occupies only the $[Pd_6]$ interstices in the hydride phase because, for example, there are 0.53 such interstices per metal atom for a disordered, random $Pd_{0.9}Rh_{0.1}$ alloy and the plateau extends to only about $r = 0.3$ at 273 K (Fig. 6). The decrease in the enthalpy for the plateau reaction must be caused by electronic band effects induced by hydrogen.

Pd–Pt alloys are an exception to the lattice contracted/expanded classification because their plateau pressures increase, and their dilute phase solubilities decrease with X_{Pt} despite the small lattice expansion of the H-free alloys. Presumably the contracted/expanded classification of behavior rests largely on the dependence of the enthalpy of hydrogen solution on the interstice size, i.e. on the lattice constant. This exceptional behavior can be partially understood; in one sense the alloys obey the contracted/expanded classification since the ΔH_H° values themselves do not change much, which is consistent with the very small change of lattice constant. The change of solubility in the dilute phase with X_{Pt} is mainly due to the effect of entropy. The plateau pressure increases with X_{Pt}, however, which does constitute an exception to the classification. This is probably inevitable if the ΔH_H° values are nearly constant, as they are for Pd–Pt, because the difference between the plateau enthalpies

and those at infinite dilution are always smaller for alloys of Pd, 'expanded or contracted', than is the difference for pure Pd. Consequently the plateau enthalpies for the Pd–Pt alloys would be expected to decrease with X_{Pt} and the plateau pressures increase.

Acknowledgements

The authors (TBF and HN) wish to acknowledge financial support from the NSF. Y. Sakamoto wishes to thank the Grant-in-Aid for Scientific Research from the Ministry of Education (Japan).

References

[1] Y. Sakamoto, U. Miyagawa, E. Hamamoto, F. Chen, T. Flanagan and R.-A. McNicholl, *Ber. Bunsenges. Phys. Chem., 94* (1990) 1457.
[2] A. Maeland and T. Flanagan, *J. Phys. Chem., 68* (1965) 1419.
[3] J.C. Barton, J.A.S. Green and F.A. Lewis, *Trans. Faraday Soc., 62* (1966) 960.
[4] B. Baranowski, F. Lewis, S. Majchrzak and R. Wiśniewski, *J. Chem. Soc. Faraday Trans. 1, 68* (1972) 824.
[5] H. Noh, W. Luo and T. Flanagan, *J. Alloys Comp., 196* (1993) 7.
[6] F. Lewis, The Palladium–Hydrogen System, Academic Press, NY, 1967.
[7] T. Flanagan and Y. Sakamoto, *Plat. Met. Rev., 37* (1993) 26.
[8] H. Noh, T. Flanagan, B. Cerundolo and A. Craft, *Scripta Metall., 25* (1991) 225.
[9] H. Noh, T. Flanagan, Z. Gavra, J. Johnson and J. Reilly *Scripta Met. Mater., 25* (1991) 2177.
[10] H. Noh, S. Luo, D. Wang, J. Clewley and T. Flanagan, *J. Alloys Comp., 218* (1995) 218.
[11] W. Oates and T. Flanagan, *Prog. Solid State Chem., 13* (1981) 193.
[12] F. Chen, M. Furukawa and Y. Sakamoto, *J. Less-Common Met., 155* (1989) 173.
[13] T. Kuji, B. Bowerman, W. Oates and T. Flanagan, *J. Phys. F:, 13* (1983) 1785.
[14] Y. Sakamoto, Y. Haraguchi, M. Ura and F. Chen, *Ber. Bunsenges. Phys. Chem., 98* (1994) 964.
[15] H. Brodowsky and E. Poeschel, *Z. Phys. Chem. N.F., 144* (1965) 143.
[16] T. Flanagan and H. Noh, *Z. Naturforsch., 50a* (1994) 475.
[17] M. Wise, J. Farr, I. Harris and J. Hirst, L'Hydrogéne dans les Mètaux, Tome 1, Ed. Sicence et Ind., Paris, 1972, p. 1.
[18] J. Lynch, J. Clewley, T. Curran and T. Flanagan, *J. Less-Common Met., 55* (1977) 153.
[19] T. Flanagan and G. Biehl, *J. Less-Common Met., 82* (1981) 383.
[20] E. Akiba, K. Nomura and S. Ono, *J. Less-Common Met., 129* (1987) 159.
[21] W. Luo, J. Clewley and T. Flanagan, *J. Less-Common Met., 179* (1993) 77.
[22] Y. Sakamoto, T. Matsuo, H. Sakai and T. Flanagan, *Z. Phys. Chem. N.F., 162* (1989) 83.
[23] R. Burch and R. Buss, *J. Chem. Soc., Faraday Trans. 1, 71* (1975) 922.
[24] A. Carson, T. Flanagan and F. Lewis, *Trans. Faraday Soc., 56* (1960) 1.